

CuAg nanoparticles on TiO₂ for high-efficiency photodegradation of acetaldehyde

XU Ji-liang¹, WANG Liu-feng², JIANG Peng-yan¹, LI Shu-hui¹, HUANG Ji-wu^{1*}, WANG Liang-bing^{1*}

(1. State Key Laboratory for Powder Metallurgy, School of Materials Science and Engineering, Central South University, Changsha 410083, China; 2. Zhejiang NHU Company Ltd., Shaoxin 312500, Zhejiang, China)

Abstract: Photodegradation of acetaldehyde serves as a novel and efficient approach for removing acetaldehyde, and TiO₂ is generally used as a photocatalyst. However, TiO₂ has a weak adsorption capacity for acetaldehyde, low product selectivity, and high electron-hole pair recombination rate, which significantly limit the treatment performance of acetaldehyde. In this study, we successfully constructed a highly active and stable photocatalyst for photocatalytic degradation of acetaldehyde by loading CuAg nanoparticles on TiO₂ (CuAg/TiO₂), which efficiently solved the inherent defects of TiO₂. The degradation rate of acetaldehyde on CuAg/TiO₂ was up to 42.49% under the irradiation of natural sunlight. CuAg/TiO₂ retained above 98.89% of initial activity after four successive rounds of full spectrum photodegradation. Further mechanism studies indicated that CuAg nanoparticles in CuAg/TiO₂ generated hot electrons under light, followed by the transfer of hot electrons to TiO₂ and oxygen adsorbed on Ag sites. The generated superoxide radicals on CuAg/TiO₂ can efficiently degrade acetaldehyde, resulting in the remarkable performance in the removal process of acetaldehyde.

Key words: silver; surface plasmon resonance; copper; acetaldehyde photodegradation; plasmonic catalysis
CLC number: O643.36 **Document code:** A **Article ID:** 1004-0676(2022)01-0001-09

TiO₂ 上的 CuAg 纳米粒子用于高效乙醛光降解 (英文)

徐佳梁¹, 王柳枫², 蒋朋宴¹, 李树蕙¹, 黄继武^{1*}, 王梁炳^{1*}

(1. 中南大学 材料科学与工程学院 粉末冶金国家重点实验室, 长沙 410083;
2. 浙江新和成股份有限公司, 浙江 绍兴 312500)

摘要: 光降解乙醛(CH₃CHO)是一种新型高效的乙醛去除方法, 通常采用 TiO₂ 作为光催化剂。然而 TiO₂ 对乙醛吸附能力较弱, 对产物的选择性较低, 电子-空穴对重组率较高, 严重限制了对乙醛的降解性能。本研究通过在 TiO₂ 上负载 CuAg 纳米粒子(CuAg/TiO₂), 成功构建了高效稳定的光催化降解乙醛催化剂, 有效解决了 TiO₂ 的固有缺陷。在自然光照射下, CuAg/TiO₂ 对乙醛的降解率高达 42.49%。连续 4 轮全光谱光催化降解乙醛, CuAg/TiO₂ 活性均保持在 98.89% 以上。进一步的机理研究表明, CuAg/TiO₂ 中的 CuAg 纳米粒子在光照下产生热电子, 随后热电子转移到 TiO₂ 和吸附在 Ag 位点上的氧中。CuAg/TiO₂ 上生成的超氧自由基能有效地降解乙醛, 从而在乙醛降解过程中表现出优异的性能。

关键词: 银; 表面等离子共振; 铜; 乙醛光降解; 等离子共振催化

收稿日期: 2021-07-16

基金项目: 国家自然科学基金项目(51801235 和 51674303); 中南大学创新驱动项目(2018CX004); 中南大学启动资金项目(502045005)

第一作者: 徐佳梁, 男, 硕士研究生。研究方向: 乙醛光降解。E-mail: xujl9999@csu.edu.cn

*通信作者: 王梁炳, 男, 博士, 教授。研究方向: 有色金属催化。E-mail: wanglb@csu.edu.cn

黄继武, 男, 教授。研究方向: 有色金属冶金。E-mail: huangjw@csu.edu.cn

Acetaldehyde, as a volatile organic chemical, is one of the typical air pollutants^[1]. Especially in the modern residential and commercial buildings, cars and other indoor spaces, the concentration of acetaldehyde is often higher than outside. Long-term inhalation of acetaldehyde pollutants could cause a range of symptoms, including headache, nausea, and even damage of liver's function^[2-3]. Currently, many techniques, such as physical adsorption, biodegradation, thermal catalysis technology, and photocatalytic oxidation, have been used to remove acetaldehyde pollutant^[3-4]. Among them, photocatalysis has become one of the most effective techniques for acetaldehyde removal because of its non-toxic, low cost, convenient operation, and eco-friendly^[3]. Titanium dioxide (TiO₂) with semiconductor properties is widely used in photocatalytic degradation of air pollutants^[5-18]. However, its application on degrading acetaldehyde has some limitations due to the inherent defects of TiO₂^[6, 8, 11]. For instance, TiO₂ has low acetaldehyde adsorption capacity, low product selectivity and high electron-hole pair recombination rate^[13, 15, 18]. Thanks to the multitudinous efforts of several research groups, it has been found that the synergistic catalytic effect between plasmonic metals and semiconductors can effectively improve its photodegradation efficiency^[4, 19-20]. For example, Jia and co-workers^[4] proposed a heterogeneous catalyst consisting of plasmonic gold nanoparticles and TiO₂ for removing acetaldehyde. The synergistic effect enhances the photodegradation efficiency of acetaldehyde from two main aspects: 1) the presence of TiO₂ particles leads to the enhancement of localized electric fields on the plasmonic surfaces, causing the enhanced adsorption of acetaldehyde and reaction intermediates on catalyst surfaces, and also changing its product selectivity. 2) The interaction between the plasmonic particles and TiO₂ particles promotes the separation of photogenerated carriers and improves the life spans of catalysts^[4, 20].

We reported a properly designed CuAg/TiO₂ catalyst for high-efficiency photocatalytic degradation of acetaldehyde, which showed remarkable catalytic activity for the photodegradation of acetaldehyde and also high CO₂ product selectivity. During the process of

photodegradation of acetaldehyde, the degradation rate of acetaldehyde on CuAg/TiO₂ was up to 98.97% under the irradiation of 385 nm light. Impressively, CuAg/TiO₂ had an acetaldehyde degradation rate of 42.49% under the irradiation of natural sunlight. Furthermore, more than 98.89% of initial activity was maintained after four catalytic cycles. Further mechanism studies indicated that oxygen adsorbed on Ag sites obtained hot electrons generated by the localized surface plasmon resonance (LSPR) effect and then formed superoxide radicals, while TiO₂ efficiently adsorbed acetaldehyde molecules on CuAg/TiO₂, directly contributing to the performance improvement of CuAg/TiO₂.

1 Experiments

1.1 Materials and chemicals

Silver nitrate (AgNO₃) was purchased from Sinopharm Chemical Reagent Co. Ltd. Copper nitrate trihydrate (Cu(NO₃)₂·3H₂O) was obtained from Shanghai Aladdin Biochemical Technology Co. Ltd. Hydrazine hydrate (N₂H₄·H₂O, 80%) was supplied by Hunan Huihong Chemical Reagent Co. Ltd. Commercial P25 powder was purchased from Degussa company. High purity carbon dioxide (CO₂ ≥99.999%) was ordered from Saizhong Specail Gas Co. Ltd. All aqueous solutions were prepared using deionized (DI) water with a resistivity of 18.2 MΩ·cm⁻¹.

1.2 Synthesis of Cu/TiO₂, Ag/TiO₂ and CuAg/TiO₂

All catalysts were prepared *via* hydrazine hydrate reduction method. In general, the synthesis of Cu/TiO₂ catalysts is as follow: 1 g of TiO₂ was dispersed in 5 mL of Cu(NO₃)₂ solution (63 μmol/L), then stirred the mixture for 3 h in a 20 mL reaction flask at 80°C, and dropwisely added hydrazine hydrate into the mixture and stirred for another 1 h at 80°C; and washed the resulted precipitates with deionized (DI) water and centrifuged for several times. The obtained Cu/TiO₂ was dispersed in DI water for further use. The preparation methods of Ag/TiO₂ and CuAg/TiO₂ were similar to that of Cu/TiO₂, except that 1 g of TiO₂ was dispersed in 5 mL of AgNO₃ (37 μmol/L) solution or a solution of AgNO₃ (23.3 μmol/L) and Cu(NO₃)₂ (23.3 μmol/L).

1.3 Photocatalytic tests

The photocatalytic degradation of acetaldehyde was conducted in a 352 mL quartz topirradiation-type reaction vessel. First, 100 mg of catalysts was evenly spread on the bottom of reaction vessel by gradually spraying the suspended catalyst mixture into the reactor, then injected acetaldehyde gas ($\sim 400 \times 10^{-6}$) into the reactor. In order to achieve adsorption-desorption equilibrium between acetaldehyde and the photocatalyst, the reactor was kept under dark for 2 hours. After illumination, the concentration of acetaldehyde in the reactor was monitored at set intervals by a gas chromatography (GC) (9790II, FULI) equipped with a flame ionization detector (FID). The acetaldehyde degradation (X , %) was calculated by the formula:

$$X = (C_0 - C) / C_0 \times 100\% \quad (1)$$

where C_0 and C represent the initial concentration and real-time concentration of acetaldehyde, respectively.

1.4 Characterization

The XRD patterns were obtained by a Rigaku X-ray diffractometer (Rigaku, MiniFlex 600) with Cu-K α radiation ($\lambda = 1.54178 \text{ \AA}$). TEM and HAADF-STEM

images were obtained on a field-emission transmission electron microscope (JEOL, ARM-200F) with an acceleration voltage of 200 kV. X-ray photoemission spectroscopy (XPS) experiments were implemented at BL10B beamline in the National Synchrotron Radiation Laboratory (NSRL) in Hefei, China. The UV-Vis absorption experiments were carried out on a double beam UV-Vis spectrophotometer (Persee, TU-1901) at room temperature. The inductively coupled plasma optical emission spectrometry (ICP-OES) experiments were implemented on a plasma spectrometer (Spectro, Spectro Blue SOP). The CO₂ concentration during the photodegradation of acetaldehyde was investigated using a gas chromatography (GC) (9790II, FULI) equipped with a thermal conductivity detector (TCD).

2 Results and discussions

2.1 Structure characterizations of photocatalysts

The samples were characterized by TEM, HAADF-STEM, and EDX elemental mapping, as shown in Fig.1.

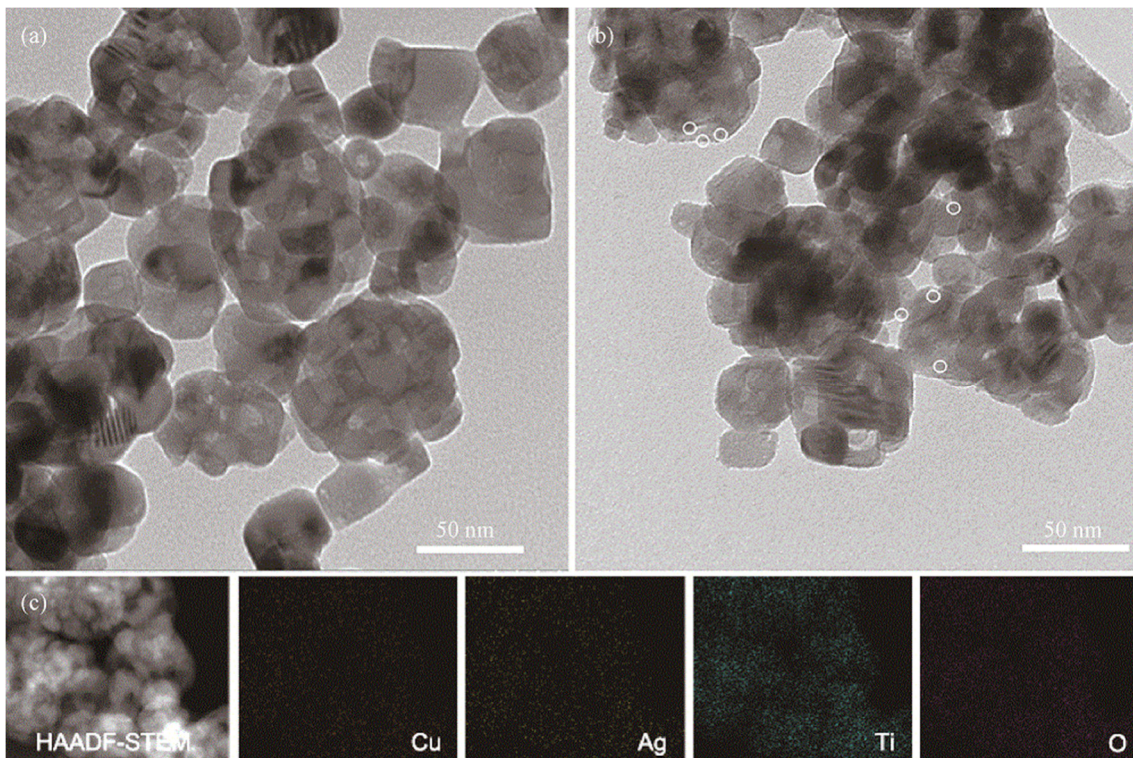


Fig.1 TEM images of (a) TiO₂, (b) CuAg/TiO₂ and (c) HAADF-STEM and the corresponding EDX elemental mapping images of CuAg/TiO₂

图 1 TiO₂(a)和 CuAg/TiO₂(b)的透射电子显微镜图像及 CuAg/TiO₂ 的 HAADF-STEM 及相应的 EDX 元素映射图(c)

Fig.1(a) showed the TEM image of TiO_2 , where the average particle size of TiO_2 was ~ 50 nm. Fig.1(b) illustrated the TEM image of CuAg/TiO_2 prepared *via* hydrazine hydrate reduction method. Isolated metal nanoparticles with extremely small sizes were marked with white circles, and metal nanoparticles uniformly distributed on the surface of TiO_2 nanoparticles. HAADF-STEM image and the corresponding energy dispersive X-ray (EDX) elemental mapping of CuAg/TiO_2 showed that Cu, Ag, Ti, and O elements evenly distributed in the nanostructure (Fig.1(c)).

The crystalline structures and compositions of the as-synthesized samples were further analyzed by X-ray diffraction (XRD). As shown in Fig.2, the main lattice type of TiO_2 nanoparticles was anatase. As for Cu/TiO_2 , Ag/TiO_2 , and CuAg/TiO_2 , the characteristic peaks of Cu and Ag were weak, which might be due to the amorphous Cu, Ag, and CuAg nanoparticles. The XRD results agreed with the analysis of TEM images.

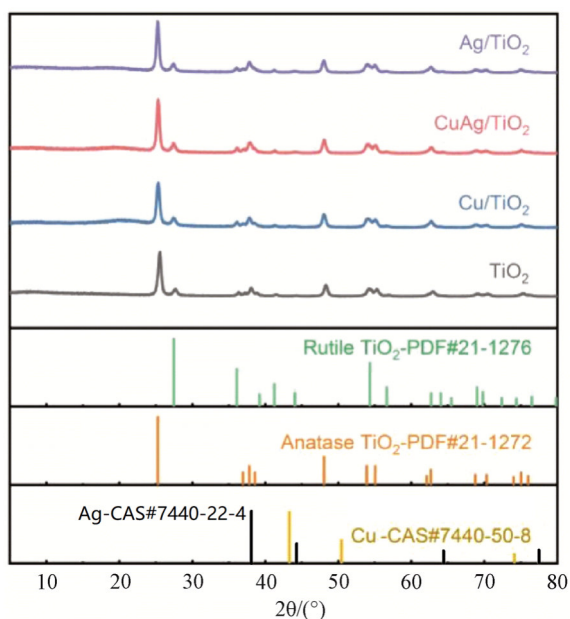


Fig.2 XRD patterns of samples

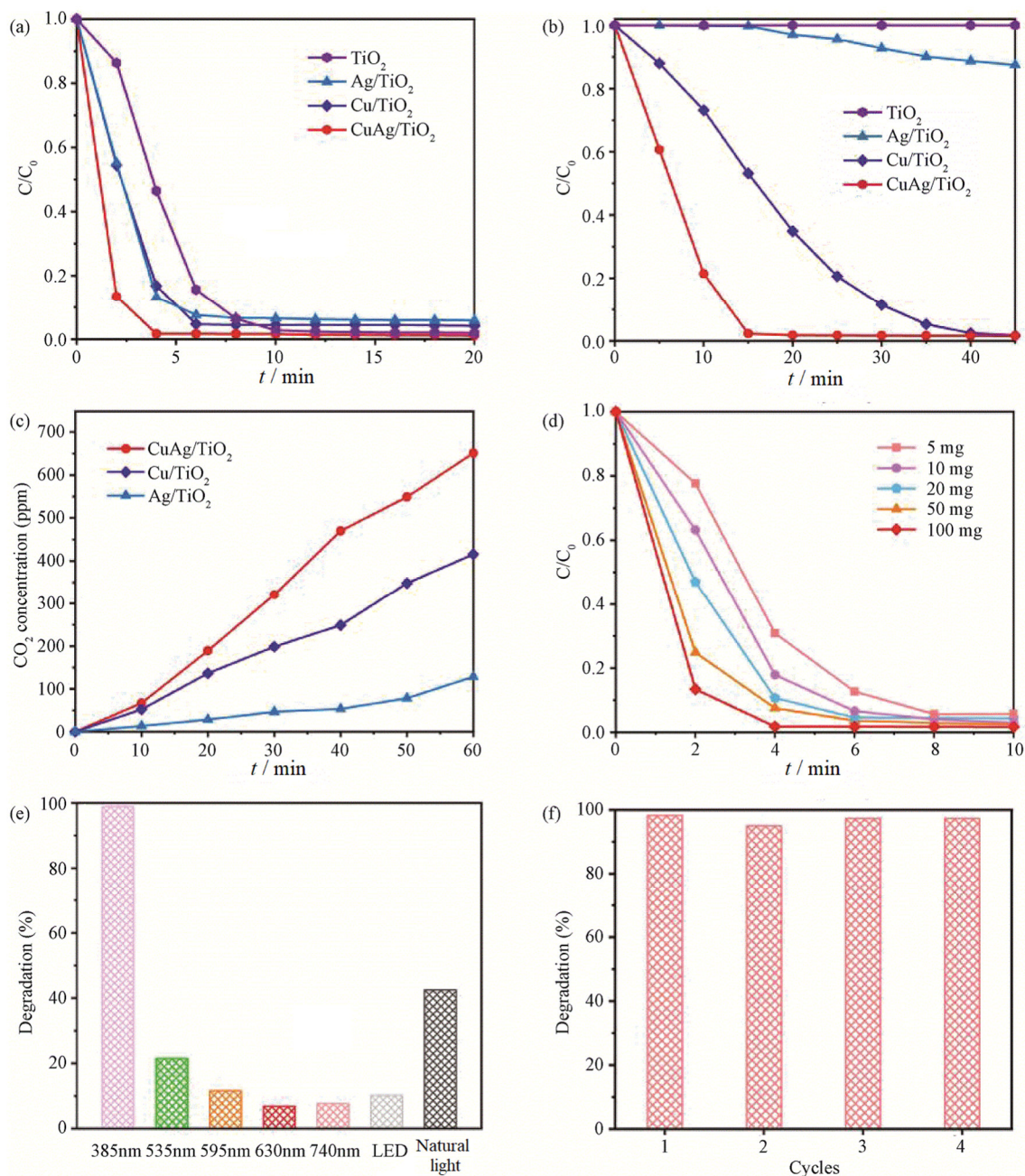
图 2 样品的 X 射线衍射图谱

2.2 Catalytic performances of photocatalysts in the degradation of acetaldehyde

The catalytic performances of as-obtained Cu/TiO_2 , Ag/TiO_2 , CuAg/TiO_2 , and TiO_2 in photocatalytic degradation of acetaldehyde were evaluated, and the experimental methods were described in the

Experiments section. A blank test was conducted without any catalyst, and no product was observed.

Fig.3(a) illustrated the reaction profiles of TiO_2 , Ag/TiO_2 , Cu/TiO_2 and CuAg/TiO_2 versus time during photocatalytic degradation of acetaldehyde. CuAg/TiO_2 attained the highest acetaldehyde conversion rate of 98.84% within 20 minutes. In comparison, the degradation rates of acetaldehyde on Cu/TiO_2 , Ag/TiO_2 , and TiO_2 reduced to 95.76%, 94.11%, and 98.08% under the same conditions, respectively. The photocatalytic activities of as-obtained catalysts under visible light ($\lambda > 400$ nm) irradiation were evaluated. As shown in Fig.3(b), the acetaldehyde concentration on CuAg/TiO_2 was quickly decreased, reaching a turning point at about 15 min, and a acetaldehyde conversion rate of 98.36% was obtained within 45 min. The catalytic performance of Cu/TiO_2 was similar to that of CuAg/TiO_2 , and its acetaldehyde conversion rate reached to 98.24%. The catalytic performances of Ag/TiO_2 and TiO_2 were far inferior to Cu/TiO_2 and CuAg/TiO_2 , only 12.52% and nearly 0 conversion rate under visible light irradiation were obtained, respectively. To explore reaction path of acetaldehyde photodegradation, we collected products during reaction. Fig.3(c) showed the time function of generating CO_2 from the photodegradation of acetaldehyde under visible light irradiation. There was no CO_2 released on TiO_2 catalyst, and the amount of produced CO_2 also followed the order of $\text{CuAg/TiO}_2 > \text{Cu/TiO}_2 > \text{Ag/TiO}_2$. When the reaction time was 60 min, the concentration of CO_2 on CuAg/TiO_2 catalyst reached to 651.42×10^{-6} , which was much higher than that of other catalysts. Fig.3(d) revealed that the conversion rate of acetaldehyde increased with catalyst mass. The effects of different wavelengths of light irradiation on acetaldehyde degradation were investigated. As shown in Fig.3(e), CuAg/TiO_2 had an optimal degradation rate of 98.97% under the light wavelength of 385 nm, which was much higher than that of other wavelengths. Impressively, the degradation rate of acetaldehyde on CuAg/TiO_2 was up to 42.49% under the irradiation of natural sunlight, which was of great significance for practical application.



(a). Full spectrum of Xenon lamp (氙灯全光谱); (b). Visible light (可见光 $\lambda > 400$ nm); (c) Time course of CO₂ production under visible light irradiation (可见光照射下产生 CO₂ 的时间过程); (d). Time course over different amount of CuAg/TiO₂ (不同 CuAg/TiO₂ 量的时间历程); (e). Photocatalytic degradation of acetaldehyde on CuAg/TiO₂ under the irradiation of different light (不同光照射下 CuAg/TiO₂ 光催化降解乙醛的时间历程); (f). Cyclic tests of photocatalytic degradation of acetaldehyde on CuAg/TiO₂ under full spectrum irradiation (全光谱照射下 CuAg/TiO₂ 光催化降解乙醛的循环试验)

Fig.3 Time course under irradiation

图 3 光照下反应时间历程

The cyclic catalytic performance of CuAg/TiO₂ photocatalyst was tested. As shown in Fig.3(f), CuAg/TiO₂ retained more than 98.89% of the initial activity after four successive rounds, indicating its excellent stability. In brief, CuAg/TiO₂ showed a good applicability in the photocatalytic degradation of

acetaldehyde.

Besides the degradation of acetaldehyde, we also evaluated the catalytic performances of CuAg/TiO₂ and TiO₂ for the photodegradation of benzene. As shown in Fig.4(a), both CuAg/TiO₂ and TiO₂ exhibited catalytic activities under full spectrum irradiation of xenon lamp.

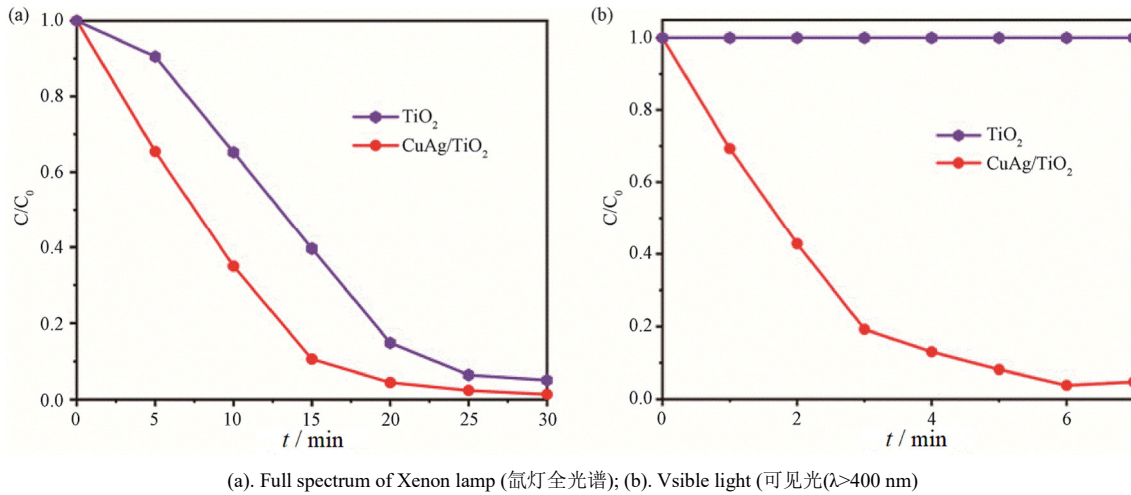


Fig.4 Time course of photocatalytic degradation of benzene on CuAg/TiO₂, and TiO₂ under irradiation

图 4 CuAg/TiO₂ 和 TiO₂ 光催化降解苯的时间历程

The degradation rate of benzene on CuAg/TiO₂ was higher than that of TiO₂, which reached to 98.63% within 30 minutes. Under the irradiation of visible light, there was no activity on TiO₂ catalyst, while the optimal conversion rate on CuAg/TiO₂ was 96.15% (Fig.4(b)). Thus, CuAg/TiO₂ catalyst can be extended to photodegradation of benzene in the air.

2.3 Mechanism studies of excellent catalytic activity for CuAg/TiO₂ in photocatalytic degradation of acetaldehyde

In order to elucidate the mechanisms of the remarkable catalytic activity of CuAg/TiO₂ in photodegradation of acetaldehyde, we investigated its optical and electronic structure.

Fig.5(a) showed the diffuse reflectance ultraviolet-

visible (UV-Vis) spectra, where CuAg/TiO₂ and Ag/TiO₂ exhibited similar optical properties with strong absorption in the full spectrum of 300~750 nm. A broad characteristic plasmonic absorption band of CuAg/TiO₂ at ~510 nm was clearly observed, while that of Ag/TiO₂ was showed at ~490 nm. In contrast, Cu/TiO₂ had no such characteristic absorption band in the visible light region while the absorbance of light was constantly enhanced. It can be inferred that CuAg/TiO₂ had the effects of both Ag/TiO₂ and Cu/TiO₂, resulting in the high absorption at about 510 nm. The absorbance of CuAg/TiO₂ in the visible light region was much higher than that of Ag/TiO₂, resulting in the outstanding degradation rate of acetaldehyde on CuAg/TiO₂ catalyst under visible light irradiation.

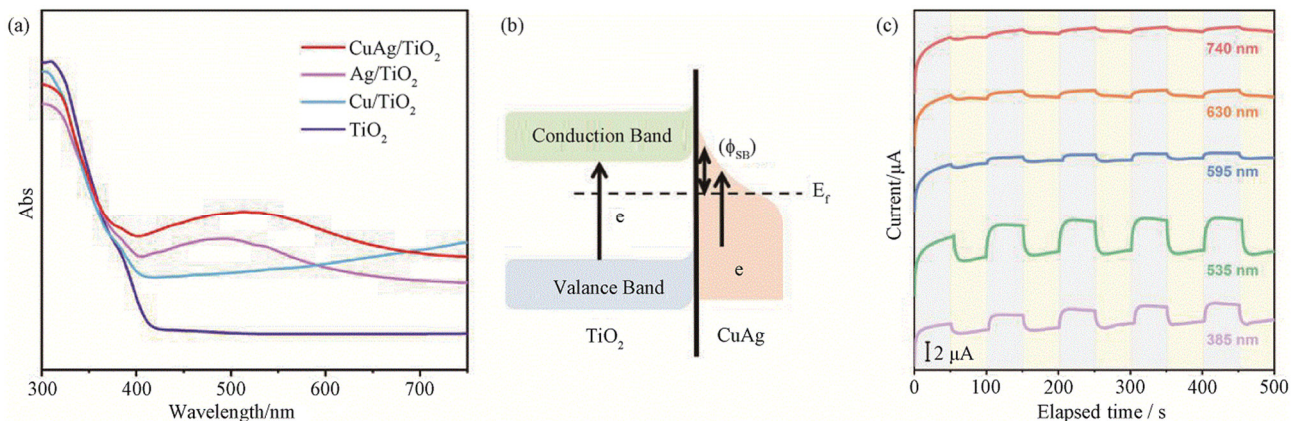


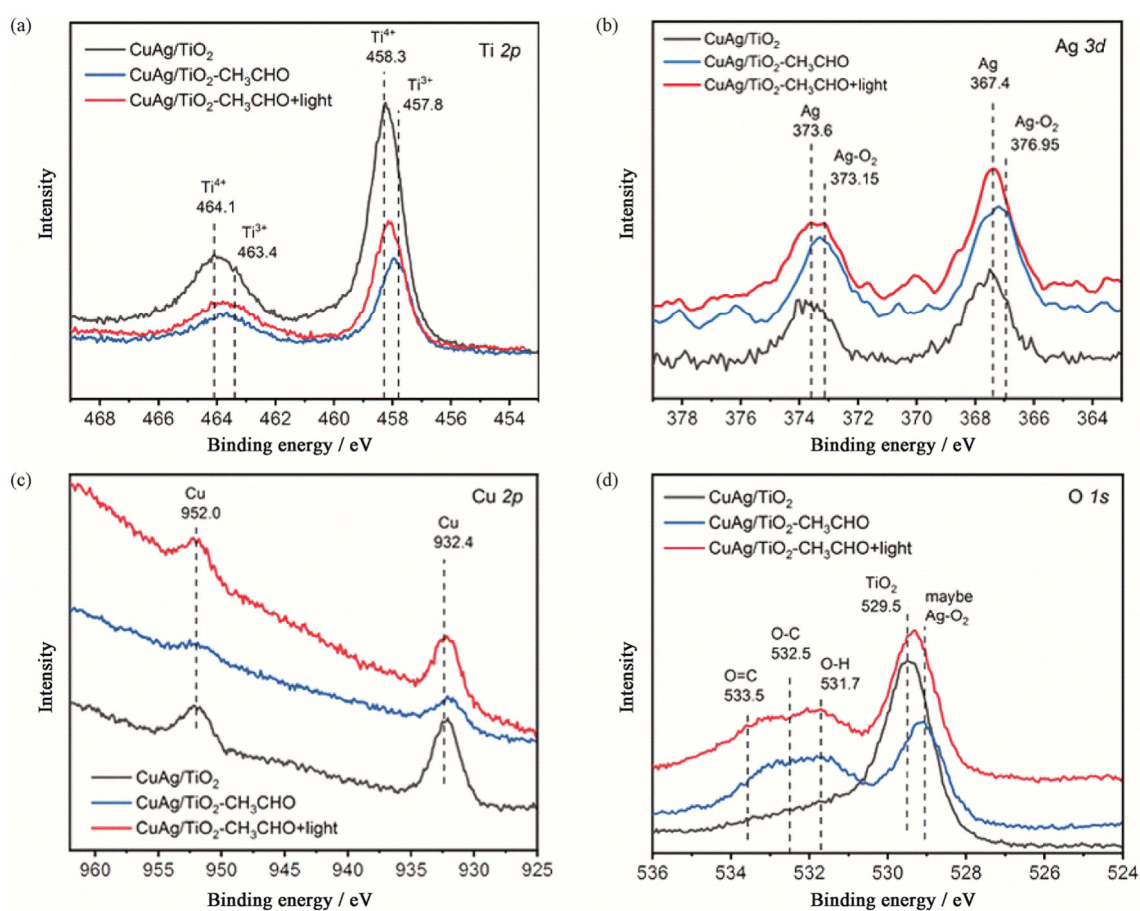
Fig.5 (a). UV-Vis absorption spectroscopy; (b) Schematic diagram of the indirect charge-transfer mechanism on CuAg/TiO₂; (c) Transient photocurrent responses of CuAg/TiO₂ under irradiation of different wavelengths of light

图 5 (a). 紫外-可见吸收光谱; (b). CuAg/TiO₂ 间接电荷转移机理示意图; (c). CuAg/TiO₂ 在不同波长照射下的瞬态光电流响应

In addition, a Schottky barrier was created at the interface between CuAg nanoparticles and TiO₂ (Fig.5(b)). The hot electrons generated by the LSPR effect can transfer to the conduction band of TiO₂ phase, and enter into lowest unoccupied molecular orbital (LUMO) of the adsorbed acetaldehyde through an indirect charge-transfer mechanism^[21]. The absorbed acetaldehyde molecules were activated, leading to the next level chemical transformation. Fig.5(c) revealed the changes of photocurrent on CuAg/TiO₂ catalyst under the irradiation of monochromatic light across

385~740 nm. The highest photocurrent signal located at 535 nm, which agreed with the results of UV-Vis absorption spectra. Even under the irradiation of monochromatic light of 740 nm, the signal of photocurrent was also observed.

In order to verify the electrons transferring process and the reaction intermediates of photodegrading acetaldehyde, we analyzed the *in situ* X-ray photoelectron spectroscopy (XPS) spectra of CuAg/TiO₂ during reaction process (in Fig.6).



(a). Ti 2p; (b). Ag 3d; (c). Cu 2p; (d). O 1s

Fig.6 *In situ* XPS spectra of CuAg/TiO₂ with/without light irradiation or CH₃CHO

图 6 有光照及无光照、有甲醛及无甲醛时 CuAg/TiO₂ 的原位 X 射线光电子能谱

As displayed in the Ti 2p XPS spectra of CuAg/TiO₂ (Fig.6(a)), a peak of Ti⁴⁺ appeared in the CuAg/TiO₂ catalyst, which was corresponding to TiO₂^[22]. After adding acetaldehyde, a peak of Ti³⁺ appeared in the sample without light irradiation, which was presumed to be the peak of acetaldehyde adsorbed on the Ti sites (Ti-C). The peak of Ti³⁺ disappeared

under illumination, indicating the change of Ti-C into TiO₂ owing to the conversion of acetaldehyde. The Ag 3d XPS spectra (Fig.6(b)) showed the peak binding energy of the oxygen adsorbed on the Ag sites was 376.95 eV without illumination. The peak of Ag-O₂ changed back to the peak of Ag, indicating that O₂ on Ag sites was reacted under light irradiation. In the

absence of light, acetaldehyde molecules and oxygen were attached to the surface of the catalyst, so the oxygen got hot electrons from Ag sites to form superoxide radicals that reacted quickly with acetaldehyde molecules to produce carbon dioxide [20]. As shown in the Cu 2p XPS spectra (Fig.6(c)), the valence state of Cu did not change significantly before and after lighting, indicating that Cu was indeed light absorption units that generated a lot of hot electrons by the LSPR effect under light irradiation rather than active sites. Hot electrons generated by the LSPR effect could activate acetaldehyde molecules and produce superoxide radicals. The O 1s XPS spectra of CuAg/TiO₂ (Fig.6(d)) exhibited that there were three peaks whose binding energy was respectively corresponding to C=O, C-O and O-H under illumination, manifesting that the products of the photodegradation of acetaldehyde at least had CO₂, while other products need to be further confirmed^[23-27].

The reaction process and product compositions of photodegrading acetaldehyde were further verified by *in situ* diffuse reflectance infrared Fourier transform (DRIFT) measurement. As shown in the DRIFT spectra (Fig.7), the inverted peaks indicated that CH₃CHO was consumed during the reaction process. The absorption peaks which were corresponding to OH, CO₂, and C=C species appeared at the same time^[28]. After 10 minutes reaction under light irradiation, the amount of OH species in the product significantly increased compared

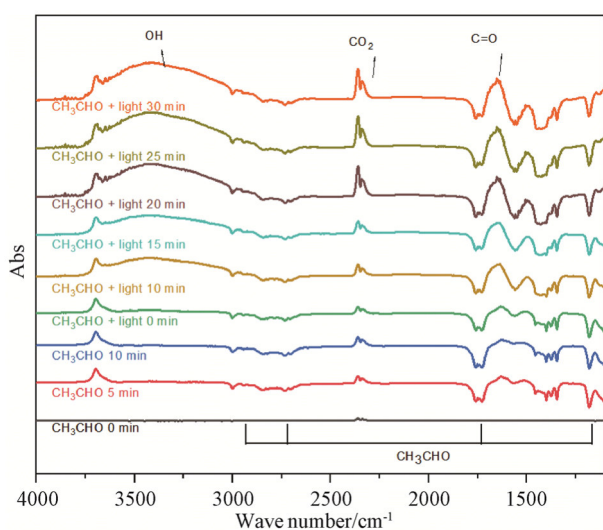


Fig.7 *In situ* DRIFT spectra for CuAg/TiO₂

图 7 CuAg/TiO₂ 的原位漫反射红外傅里叶变换光谱

with that of under unilluminated condition, suggesting that acetaldehyde degradation occurred rapidly under light irradiation. Cu not only promoted the light absorption, but also solved the intrinsic problems of a wide band gap and short lifetime of charge carriers in TiO₂ through the indirect charge-transfer mechanism. In addition, TiO₂ efficiently adsorbed acetaldehyde molecules without light irradiation, while oxygen was absorbed on Ag sites in CuAg/TiO₂. Upon the irradiation of light, oxygen absorbed on Ag sites obtained hot electrons and transformed into superoxide radicals, which reacted with acetaldehyde quickly.

3 Conclusions

In conclusion, we reported a well-designed CuAg/TiO₂ catalyst with remarkable catalytic performance towards the acetaldehyde photodegradation. CuAg/TiO₂ exhibited a splendid catalytic performance under the full spectrum and visible light irradiation. After four cycles of catalytic experiments, CuAg/TiO₂ still retained 98.89% of the initial activity, proving that CuAg/TiO₂ had an excellent stability and was of great significance on practical application. This work not only exploits a hybrid catalyst with plasmonic metals and semiconductors to achieve an efficient performance toward photodegradation of acetaldehyde, but also opens up new possibilities for designing a series of highly efficient catalysts for removing volatile organic chemicals in the air.

References:

- [1] KATSUMATA K, HOU X, SAKAI M, et al. Visible-light-driven photodegradation of acetaldehyde gas catalyzed by aluminosilicate nanotubes and Cu(II)-grafted TiO₂ composites[J]. Applied Catalysis B - Environmental, 2013, 138/139: 243-252.
- [2] JIANG Y, AMAL R. Selective synthesis of TiO₂-based nanoparticles with highly active surface sites for gas-phase photocatalytic oxidation[J]. Applied Catalysis B - Environmental, 2013, 138/139: 260-267.
- [3] LIN W, XIE X, WANG X, et al. Efficient adsorption and sustainable degradation of gaseous acetaldehyde and o-xylene using rGO-TiO₂ photocatalyst[J]. Chemical Engineering Journal, 2018, 349: 708-718.

- [4] JIA Z, AMAL M, YANG D, et al. Plasma catalysis application of gold nanoparticles for acetaldehyde decomposition[J]. *Chemical Engineering Journal*, 2018, 347: 913-922.
- [5] TAKEUCHI M, DEGUCHI J, SAKAI S, et al. Effect of H₂O vapor addition on the photocatalytic oxidation of ethanol, acetaldehyde and acetic acid in the gas phase on TiO₂ semiconductor powders[J]. *Applied Catalysis B - Environmental*, 2010, 96: 218-223.
- [6] ZHU M, MUHAMMAD Y, HU P, et al. Enhanced interfacial contact of dopamine bridged melamine-graphene/TiO₂ nano-capsules for efficient photocatalytic degradation of gaseous formaldehyde[J]. *Applied Catalysis B - Environmental*, 2018, 232: 182-193.
- [7] ISMAIL A, BAHNEMANN D. Pt colloidal accommodated into mesoporous TiO₂ films for photooxidation of acetaldehyde in gas phase[J]. *Chemical Engineering Journal*, 2012, 203: 174-181.
- [8] HU X, HU C, QU J, et al. Photocatalytic decomposition of acetaldehyde and *Escherichia coli* using NiO/SrBi₂O₄ under visible light irradiation[J]. *Applied Catalysis B - Environmental*, 2006, 69: 17-23.
- [9] AÏSSA A, PUZENAT E, PLASSAIS A, et al. Characterization and photocatalytic performance in air of cementitious materials containing TiO₂: Case study of formaldehyde removal[J]. *Applied Catalysis B - Environmental*, 2011, 107: 1-8.
- [10] SALVADORES F, ALFANO O, BALLARI M, et al. Kinetic study of air treatment by photocatalytic paints under indoor radiation source: Influence of ambient conditions and photocatalyst content[J]. *Applied Catalysis B - Environmental*, 2020, 268: 118694.
- [11] WEON S, CHOI J, PARK T, et al. Freestanding doubly open-ended TiO₂ nanotubes for efficient photocatalytic degradation of volatile organic compounds[J]. *Applied Catalysis B - Environmental*, 2017, 205: 386-392.
- [12] JIN Z, MURAKAMI N, TSUBOTA T, et al. Complete oxidation of acetaldehyde over a composite photocatalyst of graphitic carbon nitride and tungsten(VI) oxide under visible-light irradiation[J]. *Applied Catalysis B - Environmental*, 2014, 105/151: 479-485.
- [13] REN L, HOU J, BAI J, et al. The pivotal effect of the interaction between reactant and anatase TiO₂ nanosheets with exposed {001} facets on photocatalysis for the photocatalytic purification of VOCs[J]. *Applied Catalysis B - Environmental*, 2016, 181: 625-634.
- [14] BIANCHI C, GATTO S, PIROLA C, et al. Photocatalytic degradation of acetone, acetaldehyde and toluene in gas-phase: Comparison between nano and micro-sized TiO₂[J]. *Applied Catalysis B - Environmental*, 2014, 146: 123-130.
- [15] HE G, ZHANG J, HU Y, et al. Dual-template synthesis of mesoporous TiO₂ nanotubes with structure-enhanced functional photocatalytic performance[J]. *Applied Catalysis B - Environmental*, 2019, 250: 301-312.
- [16] BOUAZZA M, LILLO M, LINARES-SOLANO A, et al. Photocatalytic activity of TiO₂-based materials for the oxidation of propene and benzene at low concentration in presence of humidity[J]. *Applied Catalysis B - Environmental*, 2008, 84: 691-698.
- [17] ANDRYUSHINA N, STROYUK O. Influence of colloidal graphene oxide on photocatalytic activity of nano-crystalline TiO₂ in gas-phase ethanol and benzene oxidation[J]. *Applied Catalysis B - Environmental*, 2014, 148/149: 543-549.
- [18] PHAM T, LEE B, LEE C, et al. The advanced removal of benzene from aerosols by photocatalytic oxidation and adsorption of Cu-TiO₂/PU under visible light irradiation [J]. *Applied Catalysis B - Environmental*, 2016, 182: 172-183.
- [19] IIHOSHI T, OHWAKI T, JHON M J, et al. Improvement of photocatalytic activity under visible-light irradiation by heterojunction of Cu ion loaded WO₃ and Cu ion loaded N-TiO₂ [J]. *Applied Catalysis B - Environmental*, 2019, 248: 249-254.
- [20] ZENG Q, XIE X, WANG X, et al. Enhanced photocatalytic performance of Ag@TiO₂ for the gaseous acetaldehyde photodegradation under fluorescent lamp[J]. *Chemical Engineering Journal*, 2018, 341: 83-92.
- [21] XIAO Y, OUYANG Y X, XIN Y, et al. Application of Ag/ZnO composite materials in nitrogen photofixation: Constructing Schottky barrier to realized effective charge carrier separation [J]. *Precious Metals*, 2021, 42(4): 47-54.
- [22] WANG Y, JIA K, PAN Q, et al. Boron-doped TiO₂ for efficient electrocatalytic N₂ fixation to NH₃ at ambient conditions[J]. *ACS Sustainable Chemistry. Engineering*, 2019, 7: 117-122.